ELSEVIER

# Pressure-Sensitive Paint in Aerodynamic Testing

**B. G. McLachlan**
**J. H. Bell**
*NASA Ames Research Center*
*Advanced Aerodynamic Concepts Branch*
*Moffett Field, California*

■ Pressure-sensitive paint (PSP) is a relatively new aerodynamic measurement tool with the unique capability of providing a field measurement of pressure over a test surface. An introductory review of this technology is presented, which is confined to the application of the PSP method to aircraft development wind tunnel testing. This is at present the primary application area and thus the focus of research on the use of the method, and is the authors' own area of research. Described are PSP fundamentals, the various elements comprising PSP technology, and current limitations and considerations in applying this technology. Experimental results are presented to illustrate the present capability of the method. The few publications currently available on this subject in the open literature are also referenced.

**Keywords:** *aerodynamic measurement technique, surface pressure measurement, pressure-sensitive paint, pressure-indicating paint, photoluminescence oxygen quenching*

## INTRODUCTION

Surface pressure measurement is of fundamental importance in the experimental study of aerodynamic problems. The conventional methods presently employed for such measurements based on pressure taps or transducers have a number of limitations. One is that their very nature limits them to providing information only at discrete points on a surface. Another is that they are time-consuming and expensive to implement. In aircraft development wind tunnel testing, for example, a pressure-instrumented aircraft wind tunnel model used for estimating surface loads costs on the order of $500,000 to $1 million to construct, the pressure taps and their installation accounting for approximately 30% of this expense.

A new approach to surface pressure measurement, the use of pressure-sensitive paint (PSP), has recently appeared that offers the potential of revolutionizing the nature of such measurements in aerodynamic testing. This method employs the oxygen sensitivity of certain photoluminescent materials in the form of a "paint," in conjunction with quantitative video and image processing techniques, to map the pressure field over aerodynamic surfaces. The PSP method has a number of advantages in comparison to the present conventional point measurement methods using pressure taps or transducers. As a pressure sensor it is unique in that it is a field measurement, pressure being measured over the entire surface of a model simultaneously at a very high spatial resolution. With pressure data available over the entire model surface, flow anomalies at any point on the surface are immediately obvious, rather than having to be deduced from discrete tap data. Without the need for a large number of pressure taps, wind tunnel models could be constructed faster and for considerably less expense. Higher Reynolds numbers would also be attainable, since the conventional installation of a large number of pressure taps reduces model strength. The cost of a PSP measurement system is small compared to that of installing even a small fraction of the pressure taps in a large wind tunnel model, and unlike taps, which must be installed in each new model, the PSP system can be reused indefinitely and the cost amortized over many tests.

The PSP method's unique capabilities and potential have aroused considerable interest in the aerospace community. In particular, there is substantial interest in the use of PSP to replace the highly instrumented and costly loads model in aircraft development wind tunnel testing by obtaining pressure data from the force model used in the early part of the development testing cycle. This approach would obviously eliminate the considerable cost of the loads model as well as the wind tunnel time needed to test it. It would also make loads data available earlier in the design cycle, speeding up the overall design process and resulting in substantial productivity advances over present-day technology.

The purpose of this paper is to provide an introduction to PSP technology. It is confined to an overall review due

Address correspondence to Dr. B. G. McLachlan, NASA Ames Research Center, Mail Stop 227-2, Moffett Field, CA 94035-1000.

*Experimental Thermal and Fluid Science* 1995; 10:470–485

655 Avenue of the Americas, New York, NY 10010

0894-1777/95/$9.50
SSDI 0894-1777(94)00123-P

to the general community's unfamiliarity with the method arising from its novelty and relative newness. Provided is a description of PSP fundamentals, technology elements comprising a PSP measurement system, and the considerations and methodology involved in acquiring and processing data. This description is confined to the application of the technique to flight vehicle development wind tunnel testing. Even though the technique is applicable over a broad range of applications in experimental fluid mechanics, historically the development of PSP technology from its conception until now has been driven by its application to aircraft development testing. This is also the authors' area of work.

## MEASUREMENT CONCEPT—GENERAL DESCRIPTION

A schematic representation of how the concept works is shown in Fig. 1. In practice the model surface is coated with an oxygen-sensitive luminescent molecule dispersed in an oxygen-permeable polymer binder and illuminated with suitable exciting radiation. The intensity of the resulting luminescence depends on the oxygen partial pressure seen by the coating molecules. Since the mole fraction of oxygen in air is a known constant, the air pressure can be readily calculated from a measurement of the luminescence intensity. In an aerodynamic test the luminescence intensity distribution that accompanies the airflow-induced pressure field over the model surface can be recorded using an imaging camera, and the image can be digitized, stored, and processed on a computer to produce a map of the model surface pressure field.

## HISTORICAL PERSPECTIVE

Only recently has the potential of the oxygen sensitivity of photoluminescent materials for surface pressure field measurement been recognized and pursued by a continually growing number of groups worldwide. The first recognition of this approach and an effort to use it occurred within the former Soviet Union at TsAGI/Moscow. This work started in the early to mid-1980s in cooperation with Moscow University [1]. A somewhat recent overall description of the TsAGI work is given by Bukov et al. [2]. Initially, these Soviet efforts were not generally known in the west, information being extremely limited in scope and distribution. The existence of Soviet PSP technology was brought to light on a wide scale in the west in February 1990 through an advertisement in *Aviation Week & Space Technology* magazine. The 1990 advertisement was the start of a commercialization effort by TsAGI of their PSP system directed to the west. These efforts were initially carried out by their western European distributor, Inteco/Italy [3], and resulted in demonstration experiments of the TsAGI system being conducted at a number of the western European aerospace companies and research establishments. Engler et al. [4, 5] report on one of these experiments that was conducted in Germany at DLR/Gottingen. Recently, Inteco/Italy has pursued the independent development and commercialization of its own PSP system.

In the United States, the feasibility of using the oxygen sensitivity of photoluminescent materials for surface pressure field measurement was first demonstrated in 1989 [6–8] in experiments conducted at the NASA Ames Research Center using a coating developed by chemists at the University of Washington. Since that initial demonstration experiment, a number of groups in the United States have been engaged in successfully employing and further developing the technique. A cooperative effort between researchers at the NASA-Ames Research Center and the University of Washington has continued development of PSP technology [6–16] for a number of aerospace applications. The Boeing Commercial Airplane Company has been using it for the study of pressure fields over various aircraft configurations. McDonnell-Douglas Aerospace has been vigorously pursuing the development and employment of pressure-sensitive paint technology [17–21] for the wind tunnel study of transport and fighter configurations. Implementation and development of the PSP method has been undertaken by the NASA-Langley Research Center. The United States Air Force Arnold Engineering and Development Center has recently started to employ PSP technology in their testing programs and to pursue a development effort [22].

To date, luminescent paint systems have been almost exclusively employed to measure surface pressures on wind tunnel models, although an attempt has been made to apply the technique to flight tests [10]. Effort has also primarily focused on static (time-averaged) pressure measurements. Initial efforts, however, at the development of PSP for unsteady applications are reported throughout the literature.

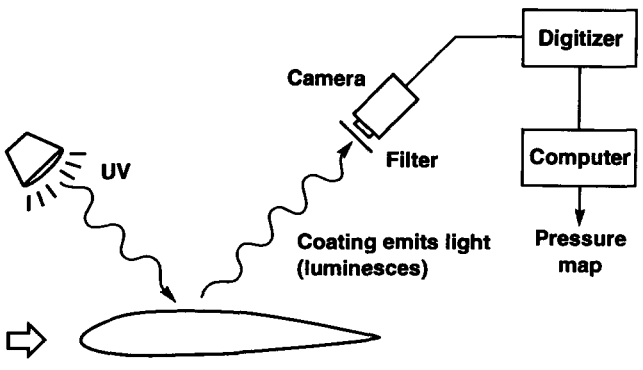


**Figure 1.** Schematic representation of PSP concept.

## PHYSICAL BACKGROUND

The paint method is based on the sensitivity of certain luminescent materials to the presence of molecular oxygen. When a luminescent molecule absorbs a photon, it is placed in an excited energy state, from which it typically returns to the ground state by emitting a new, longer wavelength photon (see Fig. 2). In some luminescent materials, however, free oxygen can initiate a side reaction that results in transition to the ground state occurring without a photon being emitted—a phenomenon known as oxygen quenching. For a given excitation level, the emitted light intensity varies inversely with the local oxygen partial pressure, and thus air pressure, since oxygen is a fixed mole fraction of air.

The oxygen quenching process can be described using the Stern–Volmer relation [23], which can be written in

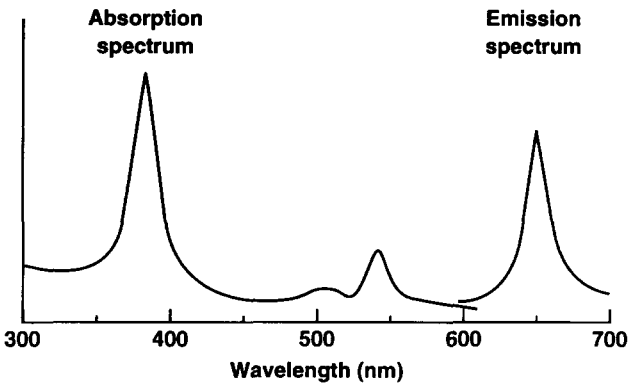


**Figure 2.** Typical PSP coating absorption/emission spectra.

the form

$$\frac{I_{\max}}{I} = 1 + Kc, \tag{1}$$

where $I$ is the luminescence intensity, $I_{\max}$ is its maximum value in the absence of quencher, $K$ is the Stern–Volmer quenching constant characteristic of the molecule, and $c$ is the concentration of the quencher, $O_2$. Both $I_{\max}$ and $K$ are functions of temperature $T$.

Most PSP coatings can be generally considered to consist of the active molecule dispersed in an oxygen-permeable binder that forms the coating structure. The relation between the oxygen concentration seen by the luminescent molecules within the coating and the pressure above the surface can be assumed to be given by Henry's law [24],

$$c = SXP, \qquad \text{where } S = S(T). \tag{2}$$

Here $S$ is the Henry's law (solubility) coefficient, $X$ is the mole fraction of oxygen in air, and $P$ is air pressure.

Using Eq. (2), the Stern–Volmer relation can be rewritten as

$$\frac{I_{\max}}{I} = 1 + KSXP. \tag{3}$$

The relationship between pressure and the resulting light emission is now explicitly clear, the luminescence intensity decreasing as the pressure increases. Unfortunately, this form of the Stern–Volmer relation is not suitable for a normal testing situation because it is not practical to determine $I_{\max}$, the maximum luminescence intensity, in the absence of quencher.

Equation (3) can be put into a form more suitable for aerodynamic testing purposes by taking the ratio of the luminescence intensity for two different flows, and hence two different quenching conditions, one with flow and the other without. This results in

$$\frac{I_0}{I} = A(T) + B(T)\frac{P}{P_0}. \tag{4}$$

Here the zero subscript denotes the value for no-flow conditions. Under such conditions $P_0$ will be uniform over the whole surface at a known constant value. The coefficients $A$ and $B$ are the coating sensitivities and are determined by an experimental calibration. As indicated, both $A$ and $B$ are functions of temperature.

In Eq. (4) the relationship between the relative intensity $I_0/I$ and the relative pressure $P/P_0$ is linear. This linearity is a result of Henry's law and its assumption that oxygen concentration is linearly proportional to pressure. For a large number of coatings and test conditions, this linear approximation is an adequate model. However, for some coatings and situations this is not the case. The diffusion of oxygen into the coating is more complex, resulting in a nonlinear relationship being displayed between $I_0/I$ and $P/P_0$. A more general form of Henry's law is required, where the Henry's law coefficient $S$ is now a function not only of temperature but also of pressure, $S = S(T, P)$. The consequence of this additional dependence is that the sensitivity coefficients in Eq. (4) will also now be functions of pressure. This multiple dependency is undesirable. In such a situation it is usual to write the Henry's law coefficient $S(T, P)$ as a polynomial expansion in pressure, the expansion coefficients being functions of only temperature. This results in a more general form of operational Stern–Volmer relation:

$$\frac{I_0}{I} = A(T) + B(T)\left(\frac{P}{P_0}\right) + C(T)\left(\frac{P}{P_0}\right)^2 + \cdots. \tag{5}$$

In practice, the second-order approximation has been found to provide an accurate description of those coatings displaying nonlinear behavior. To adequately model an unusual nonlinear response, higher order terms would be retained as needed. Note that Eq. (4) is the first-order approximation of Eq. (5).

Equations (4) and (5) are both operational forms of the Stern–Volmer relation that are suitable for aerodynamic testing. It is clear that to experimentally obtain the pressure it is necessary to acquire luminescence intensity field images under still (wind-off) and airflow (wind-on) conditions. The pressure can be readily calculated from a knowledge of $I_0$ and $I$ since $P_0$ is a known constant.

The derivation description here has been simplified to its essential elements for the purpose of clarity, and a number of important assumptions and aspects are not apparent. The first of these is that an important benefit arises from taking the ratio of the luminescence intensity field $I$ with respect to the luminescence intensity field at a reference condition, $I_0$. The result of this ratioing is that the effects of spatial nonuniformities in excitation light intensity and coating thickness are factored out. To attain this ratioing benefit it is assumed that the arrangement of the experimental geometry (the position and orientation of lamps, model, and cameras) and the excitation light intensity and distribution do not change between the acquisition of $I_0$ and $I$. A second assumption is that the excitation light intensity is low enough that the majority of the luminescent molecules are in the ground state. At high excitation intensity, a large proportion of the molecules will be in an excited state. In such conditions, near saturation the coating sensitivity coefficients will be dependent on the excitation light intensity and pressure. Finally, it should be noted that the form of Eqs. (4) and (5) does not change if $I$ and $I_0$ are at different temperatures. As long as the wind-off surface temperature is a known constant and uniform across the surface, its effect is nothing more than that of a multiplicative constant that would be incorporated into the coefficients of Eqs. (4) and (5).

## PSP CHARACTERISTICS

It must be noted that no one PSP coating formulation can be expected to work well over the diverse range of environments found in aerodynamic testing. For this reason, groups engaged in PSP technology development have leaned toward creating their own comprehensive set of PSP coatings to cover different aerodynamic conditions. One finds that the performance characteristics and photoluminescent and mechanical properties vary between coating formulations. Thus by necessity what is written here on the subject of PSP characteristics is restricted to an overall general view.

Though complex in detail, the structure of PSP coatings used for steady-pressure measurement can be considered to consist of a luminescent molecule dispersed in an oxygen-permeable matrix. At present the majority of PSP coatings appear to use some form of silicone polymer as the PSP binder matrix. All PSP formulations that we are aware of come in the form of a liquid mixture suitable for application to a surface with conventional spray-painting techniques and equipment.

The PSP coating is only one layer of a multilayer coating structure applied to the model surface. In its simpler form the PSP coating is applied over a white paint coating. More complex layered structures exist that involve the addition of multiple adhesive layers [2, 3, 5]. The white undercoat to the PSP coating is employed as an emission signal amplifier, as it significantly increases the luminescence intensity for a given excitation radiation intensity level. It accomplishes this by scattering unabsorbed exciting photons back through the PSP coating, allowing them a further chance to excite luminescent molecules, and it also reflects the emitted photons, providing a further contribution to the detected intensity.

Representative examples of PSP coating pressure dependence are shown in Fig. 3. Exhibited are the calibration curves for two different PSP coating formulations, PSP1 and PSP2, that were obtained under controlled static conditions. The data are presented in Stern–Volmer normalized form of $I_0/I$ versus $P/P_0$. The zero reference condition is in this case atmospheric. Clearly apparent in the two curves is the Stern–Volmer predicted response, luminescence intensity decreasing as pressure increases. The pressure response is nonlinear for the two coatings displayed.

PSP coatings display some characteristics that are of concern as they induce measurement error as a result of producing spatial variations in the PSP coating's response over the model surface. The magnitude of this effect depends on the specific coating formulation.

The first of these undesirable characteristics is that PSP coatings photodegrade, their response decreasing with time of exposure to excitation radiation. A photochemical reaction is produced by the excitation radiation, destroying the active molecule. An illustration of this phenomenon is shown in Fig. 4, where luminescence intensity is plotted as a function of time for the same two coatings as in Fig. 3. Depending on the coating formulation, the Stern–Volmer calibration may or may not change significantly. However, the raw emission intensity will decrease with time of exposure. Ultimately, this effect determines the useful lifetime of the PSP coating, an aspect of concern in a large-scale operational environment where time taken for coating removal and reapplication is an important issue.

The PSP1 photodegradation curve of Fig. 4 exhibits an additional phenomenon displayed by some PSP coatings, the induction effect. The coating response takes some time after exposure to excitation radiation to reach an equilibrium. In the PSP1 curve this is seen as an increase in luminescence intensity over a certain time period after exposure at $t = 0$ s to excitation radiation. There is no problem in using coatings displaying this effect for steady-state pressure measurements as long as the coating is allowed to reach its equilibrium state before data are acquired. A full description of this interesting photochemical process is given by Uibel et al. [15].

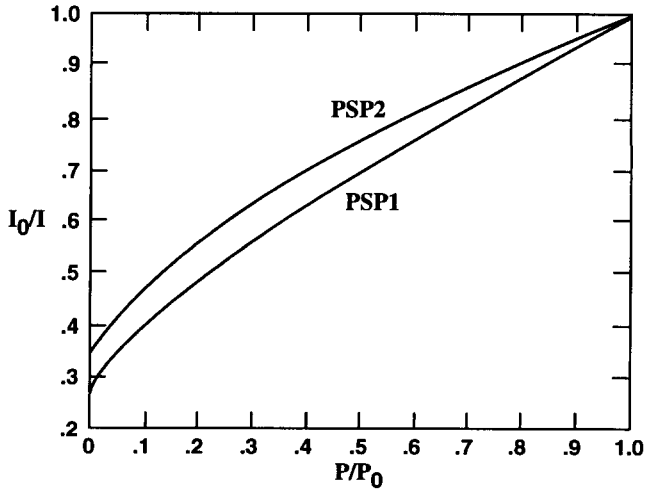


**Figure 3.** Pressure calibration curves, luminescence intensity ratio $I_0/I$ as a function of pressure ratio $P/P_0$, of two PSP coatings, PSP1 and PSP2, on a white background; $T$ = 25°C; $P_0$ = 1 atm.

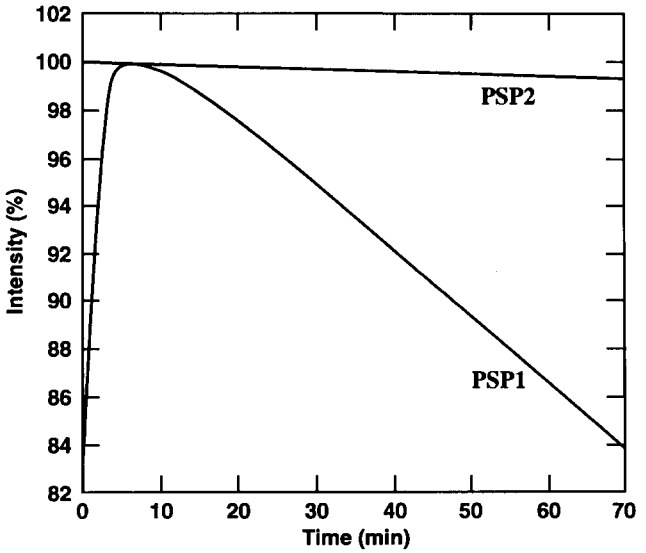


**Figure 4.** Examples of photodegradation of coating response. Two PSP coatings, PSP1 and PSP2, are shown; $T$ = 25°C; $P_0$ = 1 atm.

The plots of Figs. 3 and 4 also serve to illustrate the importance of the binder to PSP performance. The only difference between the two coatings, PSP1 and PSP2, is the coating binder; the active molecule is the same for both. As is evident, especially in the photodegradation plots of Fig. 4, the binder selection can dramatically alter the properties displayed by a PSP coating.

The second undesirable characteristic is that coating luminescence intensity exhibits a temperature dependence. This arises because of the effect of temperature on the energy state of the active molecule and the oxygen permeability of the coating. An example of this dependence is shown in Fig. 5, where the effect of temperature on the Stern–Volmer calibration curve of one of the coatings, PSP1, is displayed. The data are again presented in normalized form, $I_0/I$ versus $P/P_0$, for two different temperatures. Note that in Fig. 5 the reference condition denoted by the zero subscript was taken at a temperature of 25°C. It is clear from the two curves that the slope of the Stern–Volmer curve displays a significant variation with temperature, the emission intensity decreasing as the temperature increases. The data displayed here can be taken as an extreme example of PSP temperature dependence. However, all coatings display temperature sensitivity to some degree. In compressible flow tests where the recovery temperature over the model surface is not uniform, the coating's temperature sensitivity cannot be ignored. The character of the functional dependence of luminescence intensity on temperature can vary a great deal between different coating formulations.

## MEASUREMENT SYSTEM ELEMENTS

A PSP measurement system comprises a number of different elements. Illumination, imaging, and data acquisition/processing are system elements that require careful integration to attain a viable PSP measurement capability. Test objectives and environment determine requirement specifications of each element and the overall system. The cost and complexity of a PSP system vary dramatically depending on the test application.

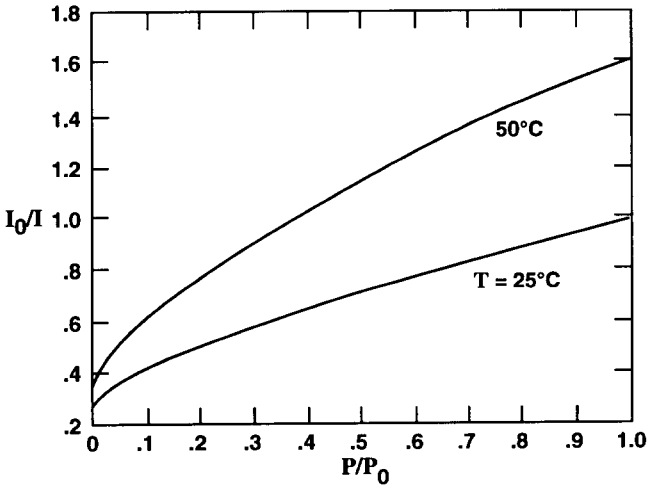


**Figure 5.** Example of effect of temperature on coating calibration curve: PSP coating PSP1 on white background; $P_0 = 1$ atm; $I_0$ for each curve was taken at 25°C.

### Illumination

The illumination portion of a PSP measurement system is used to excite the luminescent sensor molecules of the PSP coating, causing them to luminesce. The intensity of the light emitted by the coating is proportional to the excitation light that is absorbed. It is therefore necessary that the excitation light field illuminating the model surface be of sufficient power level in the PSP coating absorption wavelength band. It is also desirable, due to the wind-off and wind-on measurement methodology, that the intensity of the excitation source be stable in time. Because of the complex geometry of full aircraft configurations and test facilities, it is usually necessary to employ a number of sources to attain adequate coverage of the model surface. Spatial uniformity of the illumination field reduces errors and is desirable. It is, however, difficult to attain in many practical situations. A number of different types of excitation light sources have been employed for PSP measurements. The use of lasers in combination with fiber-optic delivery systems [2–5, 17–20], continuous and flash arc lamps [6–15, 18, 22], and incandescent lamps [16, 18, 19] has been reported. Each has advantages and disadvantages. The choice of which type of excitation source is employed depends on which PSP coating is used and the test environment. Some aspects of concern in selection are cost, performance, ruggedness, portability, and safety issues, both bureaucratic and real.

### Imaging

A wide variety of light-sensing devices can and have been used in implementation of the PSP method. These range from point detectors such as photomultiplier tubes and photodiodes to field detectors such as photographic film and electronic imaging cameras. Since the primary advantage of the method is its field measurement capability, the most effort has gone into developing that aspect. Electronic imaging cameras of the solid-state CCD type have come to be preferred in PSP applications due to their performance characteristics and the real-time processing capability they permit. Convenience, flexibility, and ease of use are also factors in this selection. As a general classification, the CCD cameras employed can be viewed as being divided into two types, conventional video and scientific grade digital cameras, which lie at opposite ends of a cost and performance spectrum. The type used is determined by the data requirements of a specific application.

**Conventional Video** Conventional black-and-white video cameras are popular in PSP applications for economic reasons. A personal computer (PC) based 8-bit resolution image acquisition and processing system using standard NTSC format video cameras can be assembled at relatively low cost owing to the vast number of commercial products available. The use of standard video has the advantage of providing real-time viewing of the image output. Displayed on a monitor, the signatures of flow structures such as shocks and vortices are easily discernible in the raw PSP image. The signal output, being standard video, can be recorded on videotape to provide a record of the test data for later analysis. Standard video cameras are robust, capable of surviving harsh test envi-

ronments. They provide reasonable spatial resolution, CCD arrays of 640 × 480 pixels being common. Unfortunately, the NTSC television format was not designed for quantitative imaging applications; consequently, standard video cameras are not precision photometric instruments. Their signal-to-noise ratio (SNR) is low, being comparable to the 8-bit resolution of the commercially available image digitizer (frame grabber) boards. Typically, they do not exhibit good response linearity, a factor of concern in the Stern–Volmer ratioing operation. However, experience has demonstrated that even with these drawbacks a standard video camera in conjunction with a PC-based 8-bit image processor does provide PSP data that are certainly acceptable for qualitative flow visualization purposes, and the pressure resolution, though poor, may be sufficient for quantitative purposes in many practical applications.

**Scientific Grade Digital** Scientific grade cooled CCD digital cameras are specifically designed for photometric applications and provide high-precision quantitative light measurements. They are designed to achieve maximum CCD performance, and they exhibit low noise, excellent linear response, and good SNR. Cameras of this type operate in a fashion similar to that of a still camera, taking an electronic snapshot, the exposure (integration) time being controlled via the host computer by the operator. Readout time of the CCD is slow, being on the order of seconds per frame, thus limiting the sampling rate. Real-time viewing of events as in standard video is not possible. Cooled CCD digital cameras offer measurements of 12–16-bit intensity resolution and high spatial resolution (e.g., 1024 × 1024 and 2048 × 2048 pixel arrays). The price of this resolution performance is that the size of the image files produced makes data transfer and storage a concern. The host computer driving the camera and storing (and even processing) the image data can range in size and capability from a PC to the highest end workstations. The primary drawback of scientific grade cameras and their associated systems is that they are expensive, their cost being significantly higher than standard video-based imaging systems. Another drawback is that these cameras are not robust, and some care must be exercised when they are employed in harsh test environments. These drawbacks are more than overcome, however, by the fact that the high quality of data produced by such imagers is a requirement in many PSP applications.

**Some Corrections** The intensity image acquired from a CCD camera contains several kinds of "noise" [25] arising from bias and random error sources. To achieve the best photometric performance from the imaging system, some corrections for bias errors have to be applied on a pixel-by-pixel basis to the raw intensity image data before further data processing procedures are performed. The two corrections of concern here, dark-level and flat-field corrections, are applied in that order to the measured raw intensity images. The luminescence intensities $I$ and $I_0$ used to derive the pressure are the final noise-corrected values. Random errors can be reduced through averaging techniques.

**Dark-Level Correction** The output value of the imaging system shows a dc offset value when no light is incident on the sensing array. This "dark noise" level is produced by CCD dark current and "noise" of the overall imaging system. So that intensity level determinations are made from a zero reference level, a dark noise level image should be acquired and subtracted from the measured raw intensity images. The dark noise level can change with time, making it advisable to obtain dark-level images just before or just after acquisition of the wind-on and wind-off raw intensity images.

**Flat Field Correction** The quantum efficiency of a CCD varies from pixel to pixel. (Put another way, there is a measurable variation in gain or responsivity from pixel to pixel.) These variations can be on the order of 2% even for a scientific grade imager. If there is no relative model movement between the wind-off and wind-on images, this responsivity variation cancels out in the Stern–Volmer ratioing process if the detector is linear. However, under conditions where there is relative model movement between images, these variations must be accounted for before the Stern–Volmer ratioing takes place. The correction procedure is to acquire an image of uniform illumination and dark level correct it. Normalizing the dark level corrected wind-on and -off intensity images with this "flat-field" image yields a corrected intensity image in which the effect of pixel gain variation is eliminated.

## Optical Filtering Requirements

It is essential that the detector record only the luminescence emission spectra—the light emitted by the PSP coating. The detection of light from sources other than the PSP coating will produce an error in the measurement. To prevent this, the use of optical filters over the detector and excitation sources is required to ensure that the wavelength of excitation illumination does not overlap with that of the luminescence emission. Optical filtering of the excitation sources allows passage of light at the absorption wavelength of the coating but prevents the transmission of light at the luminescence wavelengths that would contaminate the coating emission seen by the detector. Such filtering is necessary because all excitation sources used in PSP, with the exception of lasers, produce light over a broad wavelength band that covers not only the PSP absorption wavelength but also the emission wavelength. Optical filters over the detector permit the passage of the luminescence emission wavelengths and block other wavelengths, in particular the light produced by the filtered excitation sources.

Concern over light contamination of the luminescence signal also makes it necessary that the test section be free of extraneous sources of light at the emission wavelengths. Consequently, the standard procedure is to acquire data with the test section darkened, the only light being from the filtered excitation sources and the coating's luminescence.

## Data Acquisition / Processing

Acquisition and processing of PSP data is typically done in a modular fashion. A camera/computer system records digital images of the model under wind-on and wind-off conditions. A number of corrections and processing procedures are then sequentially applied to produce the final desired data. In the modular approach each step takes

one or more images as input and passes one or more images as output. One advantage of the modular approach is that by breaking up the computational task it simplifies it to the point where general-purpose image processing software running on a modern personal computer is more than adequate for data reduction. Several commercially available image processing packages are sufficiently flexible to allow the user to reduce PSP data. This approach is particularly well suited to small-scale research applications, where the amount of time spent reducing data is not so important and the size of the task does not preclude the use of software requiring operator interaction in the reduction process.

A more complex capability is required, however, for production tests in large-scale facilities. Two factors drive the structure of the acquisition/processing environment in that situation. The first relates to the speed of operation and automation of the data acquisition and reduction process. Since a modern large-scale production wind tunnel might take a data point on the order of every 10 s, the desire for nearly real time output puts severe demands on the processing software. The second factor is the archival and cataloging of the extremely large data sets created in production tests. In a typical test using three scientific grade CCD cameras, each with 1024 × 1024 pixel spatial resolution, image data can be generated at a rate of 18 Mbytes/min. After even a short period of testing, the PSP system operator can be faced with several gigabytes of image data to be reduced, cataloged, and archived. The automation of data acquisition and processing becomes essential. These considerations lead to the creation and use of custom software in an environment employing high-level graphics workstations and high-capacity disk arrays.

## MEASUREMENT METHODOLOGY

The structure of the measurement methodology is set by the Stern–Volmer relation, consisting of the acquisition and ratioing of two intensity field images, one at a known "wind-off" reference pressure and the other at the "wind-on" test condition. The intensity of the final ratioed image will be proportional to pressure, the scaling factor being determined through a calibration procedure to be discussed later. A practical testing situation introduces complications into the data processing procedure. To extract quantitative and accurate pressure maps from the raw image data, some corrections must be applied.

The primary cause of difficulty arises from the acquisition of the wind-off and -on images at two different times. Changes in certain factors that occur between those two times lead to error in the final pressure calculation from the image data. The main factors of concern here are differences in paint response characteristics and in model position and shape between the wind-off and -on images.

### Error Source: Model Motion and Deformation

Aerodynamic loading induces model motion and deformation at the wind-on condition that is not present at the wind-off reference condition (see Fig. 6). This motion/deformation results in spatial nonalignment of identical points on the model (Fig. 7) in the wind-on and wind-off intensity field images. Since the Stern–Volmer intensity ratio must be between the same locations on the model, not the same CCD pixels, the consequence of image nonalignment is the introduction of errors into the Stern–Volmer ratioing operation and thus the pressure measurement. The error introduced by model motion/deformation becomes increasingly significant as model scale and wind tunnel dynamic pressure increase.

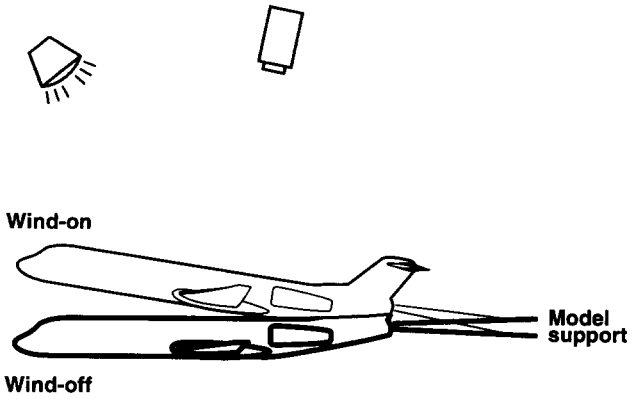


**Figure 6.** Schematic of model motion/deformation induced by aerodynamic loading.

**Registration of Wind-On and Wind-Off Images** Correction for image spatial nonalignment induced by model motion/deformation is currently done by spatially aligning, "registering," the two model images before they are ratioed. In this operation the wind-on image is aligned (i.e., shifted, rotated, scaled, warped, etc.) with the wind-off image through a mathematical transform so that a location on the model is the same in both the wind-on and -off images. The transform is usually [11, 19] a general series expansion in the wind-on image plane coordinates and takes the form

$$\begin{aligned} x &= a_{00} + a_{10}x' + a_{11}y' + a_{20}x'^2 + a_{21}y'^2 \\ &\quad + a_{23}x'y' + \cdots, \\ y &= b_{00} + b_{10}x' + b_{11}y' + b_{20}x'^2 + b_{21}y'^2 \\ &\quad + b_{23}x'y' + \cdots. \end{aligned} \tag{6}$$

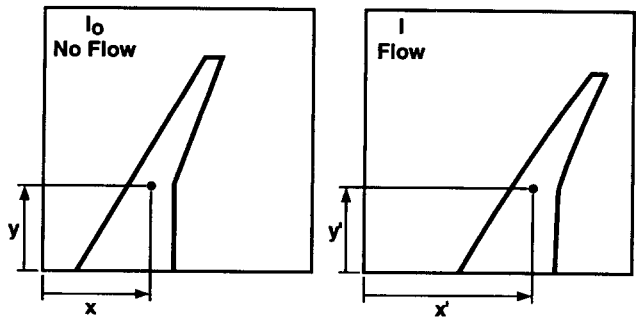


**Figure 7.** Schematic showing effect of model motion/deformation on identical points on the model in the $I_0$ and $I$ images.

The level of transform required is determined by the degree of model motion/deformation. For most wind tunnel applications involving normal configuration models it is sufficient to use the second-order biquadratic transform. Image matching within subpixel accuracy is possible. The registration procedure requires that reference marks, "control points," be placed on the model. Control points usually take the form of black circles distributed across the model. An illustration of the typical placement of control points is shown in Fig. 8. The control points are found in the wind-on and -off images, and their locations are used to determine the transform coefficients.

**Effect of Excitation Light Field Variations** Luminescence emission intensity is proportional to the excitation light that is absorbed by the coating. Consequently, variations in excitation illumination intensity incident on the model surface between the wind-off and wind-on images induce spurious emission changes that do not cancel out in the Stern–Volmer ratioing process and result in measurement error.

The illumination field can vary owing to changes over time in output of the excitation sources. In principle, the output of the excitation sources can be monitored, for example, by using a photodiode, and appropriate corrections [17, 18] applied to the recorded emission intensities. In practice, however, when using multiple excitation sources it is difficult to associate the excitation intensity incident on a given portion of the model surface with a specific source.

Changes in emission also arise as a result of model movement between wind-off and -on image acquisition. When the model moves under aerodynamic loading it moves with respect to both the imaging camera and excitation sources. Motion with respect to the camera can be corrected by image registration [11, 19]. Motion with respect to the excitation sources [2, 11] is not so easily allowed for, and a correction for this error involves spatial measurement of the incident excitation illumination field.

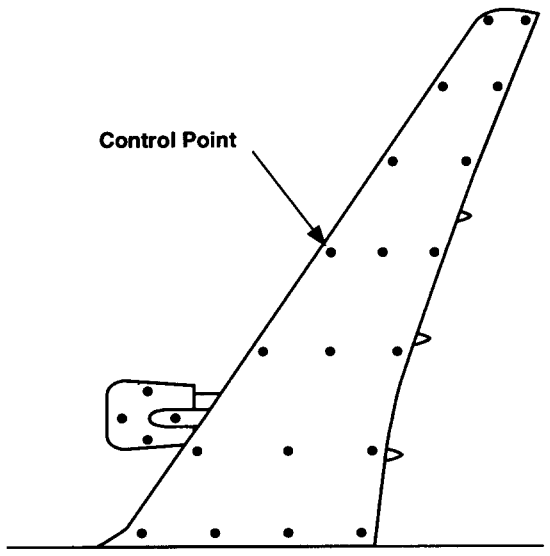


**Figure 8.** Illustration of control points (reference marks) and their typical placement on a model transport wing.

A means to correct for spatial, and also temporal, variations in the excitation field is provided by luminescent reference paints [3, 5, 17, 18] that are pressure- and temperature-insensitive and are excited and emit at the same wavelength bands as the PSP coating. They provide a measurement of excitation intensity over the surface as part of the recorded images, with the reference paint being distributed over the surface at selected discrete spots. It is usual to combine these reference spots with the control points. Interpolation is used to determine the reference level at other portions of the surface.

Another related approach is to use a multicomponent coating that incorporates a pressure-sensitive molecule and a reference luminophore that emit at different wavelengths. At the wind-on condition one camera would image the pressure signal and another camera would image the reference signal. In principle, the reference signal would contain information suitable to replace the wind-off image in the ratioing process. Multicomponent coatings incorporating a reference luminophore have the added advantage that they also provide a partial correction for the effects of airstream optical influences, such as moisture condensation, on the excitation and emission light fields.

## Mapping Data

Camera lens distortion along with perspective effects due to camera angle and model surface curvature produce spatial distortions of the model image. The result is that the final intensity ratio image is not spatially correct. For the final pressure data to be quantitatively useful, it is necessary to be able to accurately relate each point in the image plane to a corresponding point on the model surface. To do this it is necessary to map the pressure data between the two-dimensional image plane and the three-dimensional model surface (see Fig. 9). This can be viewed as an exercise in the transformation of coordinate systems. Fortunately, this is a standard problem in photogrammetry, and within that field there are a vast array of sophisticated mathematical methods to deal with it. One approach for PSP applications described by Donovan et al. [19] relies on the projective equations of photogrammetry. Another approach, described by Bell and McLachlan [11], employs the linearized form of the projective equations known as the direct linear transform. In both approaches, coefficients in the mapping transformation relations are determined using the control points and their known spatial locations. The image is mapped onto a grid that is defined in model coordinates. In its simplest form this can be a 2-D plane view representation (e.g., a wing planform view) resulting from a parallel projection of the 3-D model surface into the 2-D image plane. This 2-D representation is adequate for many quantitative uses of the pressure data. In some situations, however, a more complex form is required in which the grid is the 3-D model geometry. Surface loads estimation in aircraft design is a situation requiring such complexity.

It must be noted that the mapping of the data to model geometry, along with image registration, is the most computationally intensive portion of PSP data processing. It is absolutely necessary, however, if accurate quantitative data are required.

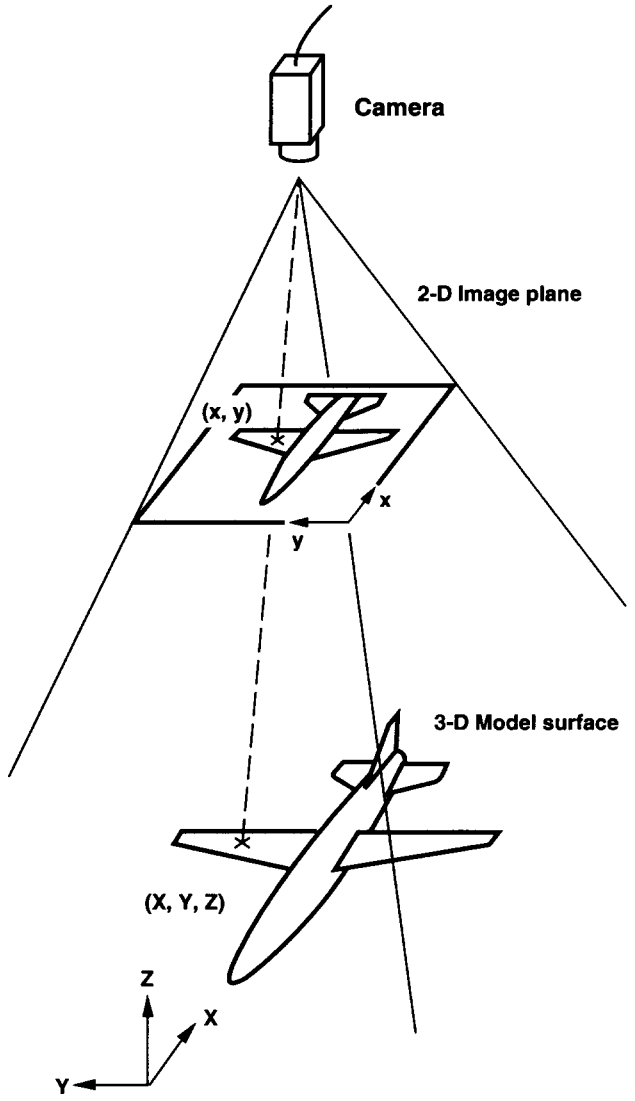


**Figure 9.** Geometry of coordinate system mapping transformation from three-dimensional model surface to two-dimensional image plane.

## Calibration

Calculation of pressure from the intensity ratio requires a determination of the sensitivity coefficients in the Stern–Volmer equation through experimental calibration of PSP coating response. Two calibration method approaches, a priori and in situ, have been employed to determine the Stern–Volmer coefficients. In both these approaches the sensitivity coefficients are obtained by a least squares fit to the Stern–Volmer equation of the measured pressures and paint intensities.

The a priori method involves the calibration of the PSP coating under static conditions. This usually takes place in a pressure- and temperature-controlled chamber on a test plate coated with the same batch of PSP and white undercoat as are applied to the model. An attractive alternative is to carry out the a priori calibration in a pressure wind tunnel where static pressure can be varied under no-flow conditions and calibration of the PSP coating on the model surface can be performed directly.

The in situ method is performed on a model equipped with pressure taps during the wind-on test condition, using data from the pressure taps and the PSP at spatially corresponding locations. The airflow-induced pressure distribution over the model surface produces the pressure range for the calibration. Accurate identification and spatial correlation of the tap and paint data requires that the in situ method be performed after the mapping operation using the spatially correct intensity ratio image.

The in situ approach would appear to negate one of the advantages of the PSP method, namely, the elimination of pressure taps and their associated cost. This is not the case; significant cost savings are still achieved by reducing the overall number of taps. The in situ approach requires relatively few taps compared to what would normally be installed in an aircraft development model, especially in a loads model.

The recovery temperature over the model surface is a factor in calibration due to the temperature dependence of the PSP coating. To correct for temperature effects, the a priori method requires a separate measurement of the model surface recovery temperature. This information along with the temperature dependence of the PSP coating pressure response curve identified from the static calibration is used to determine the appropriate sensitivity coefficient values. The in situ method does not require a separate temperature measurement because it is performed at the wind-on recovery temperature. It does require, however, that the surface be reasonably isothermal. If this is not the case and large temperature variations exist over the surface, the in situ approach fails.

**Temperature Determination** Where conditions warrant it, a number of techniques have been used to measure the surface recovery temperature to permit suitable corrections to the PSP data. Examples are thermocouples [4, 5, 17, 18] for temperature determination at selected surface points and infrared thermography [4, 5] for a full-field measurement.

Luminescent temperature-sensitive paints [2, 12, 13, 17, 18] have also been developed for this purpose. The motivation for pursuing this approach is that it has all the advantages inherent to the PSP method and can be integrated easily into the PSP measurement system. These paints have been used in a manner similar to thermocouples, with the temperature-sensitive paint placed at selected locations on the model surface, other portions of the surface being coated with PSP. In situations where the model geometry and flow display bilateral symmetry, temperature-sensitive paint and PSP have been applied to opposite halves of the model. These temperature-sensitive paints have been used alone in heat transfer studies [2, 12, 13] and to detect the location of boundary layer transition [14].

Some effort has gone into producing a dual paint formulation [12, 13, 17, 18] that permits the simultaneous field measurement of pressure and temperature. The idea is to have one coating that contains two luminescent materials that emit at different wavelengths and are excited by the same excitation source; one being primarily pressure-sensitive and the other only temperature-sensitive. The temperature-dependent signal would permit the correction of the pressure-dependent signal. The dual

pressure/temperature-sensitive coating would have the capability of permitting a complete determination of the surface thermodynamic state. This approach is being pursued by a number of developers, but so far no fully successful results have been reported.

## EXAMPLE STUDY

Here results are presented from an aircraft development wind tunnel test where the PSP method was employed. They serve to demonstrate the method's capability and to also illustrate the ratioing and registration effects described previously. The test was conducted on a generic transport wing/body configuration in the NASA Ames $11 \times 11$ ft Transonic Wind Tunnel at transonic Mach numbers from 0.7 to 0.9 and for a range of angles of attack. The model was of the half-span type, floor mounted, with a wing span of approximately 8 ft. It was extensively instrumented with multiple chordwise rows of pressure taps. Figure 10 shows the model installed in the test section. For the test, a PSP coating was applied to the wing's upper and lower surfaces. No PSP was applied to the fuselage. Control points were distributed over the wing surface to permit registration and mapping processes to be performed on the data. Excitation illumination of the PSP-coated wing surface was provided by arrays of filtered arc lamps behind windows in the test section side walls. Image data were acquired using two cooled scientific grade digital CCD cameras, one each for the upper and lower wing surfaces, with $1024 \times 1024$ pixel spatial resolution and 14-bit gray level resolution. A bandpass interference filter that passed only the luminescence emission wavelength band was placed in front of each camera lens.

**Figure 10.** Photograph of generic transport wing/body model test installation.

A representative set of measured wind-off ($I_0$) and wind-on ($I$) upper surface luminescence intensity fields for one condition are displayed in Fig. 11.* Color has been added to the images to indicate the intensity level, blue and red denoting high and low intensity levels, respectively. It is quite evident in the wind-off image that the intensity level displays a considerable spatial variation even though the pressure is uniformly constant across the surface. This variation arises from spatial nonuniformities in the excitation light intensity field and PSP coating thickness. Though not as apparent, the same degree of spatial variation exists in the wind-on image. These nonuniformity effects are factored out and eliminated by the Stern–Volmer ratioing of the two field images. The resulting intensity ratio map is directly related to the pressure field through the Stern–Volmer equation. As noted previously, airload-induced model motion and deformation introduce complications into the ratioing process. Registration of the $I$ and $I_0$ images becomes necessary.

A demonstration of the effect of image registration on the intensity ratio is provided in Fig. 12. Shown are two false-colored pressure maps calculated from the intensity ratio of the $I$ and $I_0$ images of Fig. 11, one for when the $I$ and $I_0$ images were not spatially registered and the other when the images were registered. The degree of spatial nonalignment of the $I$ and $I_0$ images is indicated in the unregistered map by the red and white bordering along the wing edges, especially prominent along the outboard portion of the wing. Comparison of the unregistered and registered maps provides an indication of the error introduced by the spatial nonalignment of the $I$ and $I_0$ images resulting from model movement and deformation. Readily apparent in the unregistered map is a considerable loss of detail in the pressure field relative to the registered map. It is worth noting that the degree of model motion and deformation displayed in the data of Fig. 12 would be considered moderate based on our experience.

Quantitative evaluation of the PSP method's accuracy is provided in Fig. 13, where PSP-derived pressures are compared to those obtained from conventional pressure taps. The PSP data are from a line next to one of the upper surface chordwise pressure tap rows. Calibration of the PSP data was accomplished using the in situ procedure described previously. The wing surface was assumed to be isothermal. As can be seen, good agreement is shown between the two measurements. This level of agreement is indicative of what can be achieved from the PSP method at present in a production environment.

A further demonstration of PSP method capability is given in Fig. 14. Shown are upper surface pressure maps for an angle of attack sweep at one fixed Mach number. It is clear from this map composite that as a quantitative measurement tool the PSP method provides vastly more complete surface information than is available from spatially discrete tap data. Also clear from Fig. 14 is the method's value as a qualitative flow visualization tool. The

* Due to the highly proprietary nature of the test results, only qualitative results are presented in Figs. 11–14. Though the absolute level is not presented, the data is linearly scaled in Figs. 11–14.

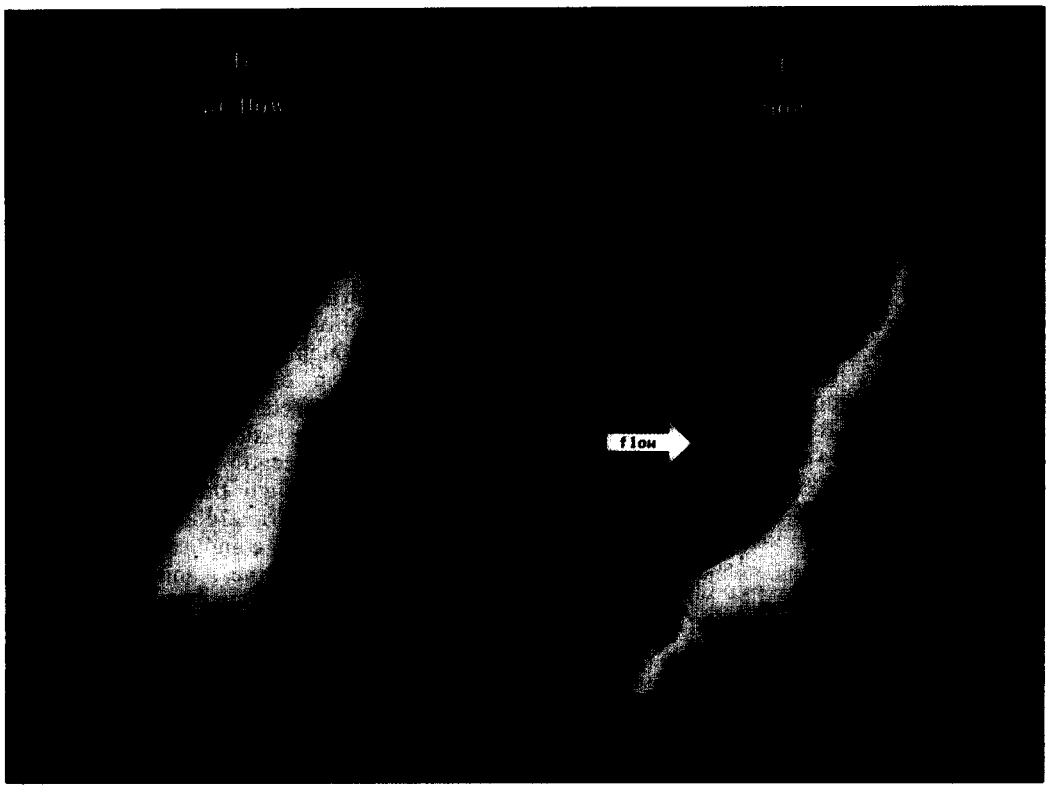


**Figure 11.** Upper surface $I_0$ and $I$ luminescence intensity field maps for $M = 0.8$ and $\alpha = 10°$. Color denotes intensity level, blue and red indicating high and low intensity, respectively.

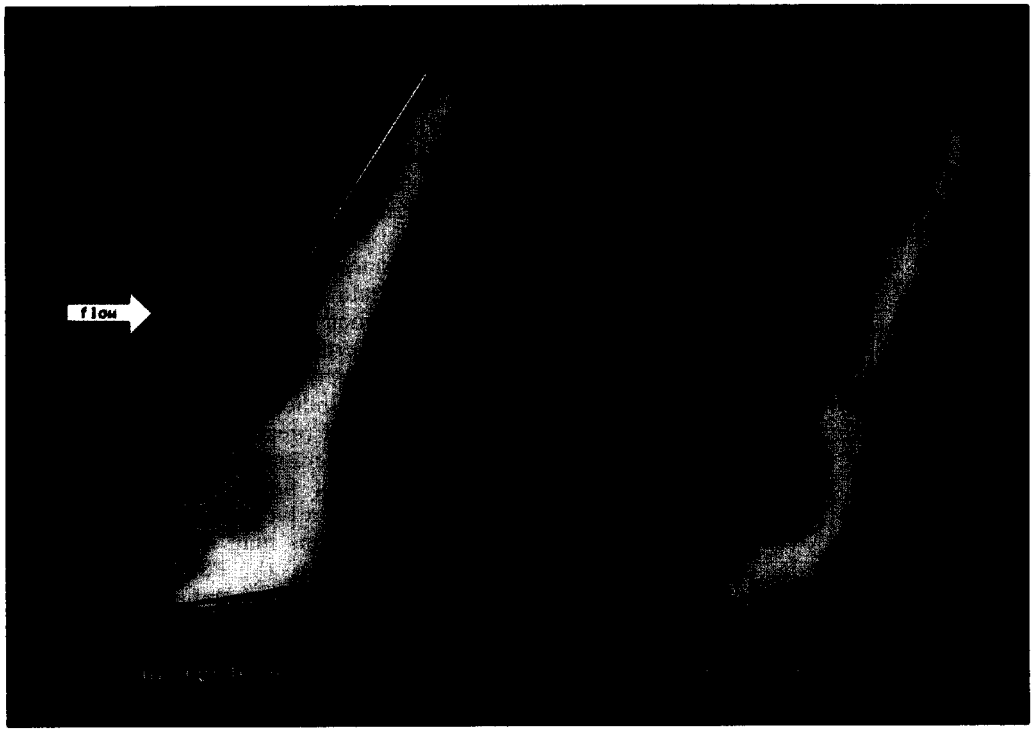


**Figure 12.** Effect of image registration. Ratio of $I_0$ and $I$ maps of Fig. 11; unregistered and registered $I_0/I$ maps are shown.

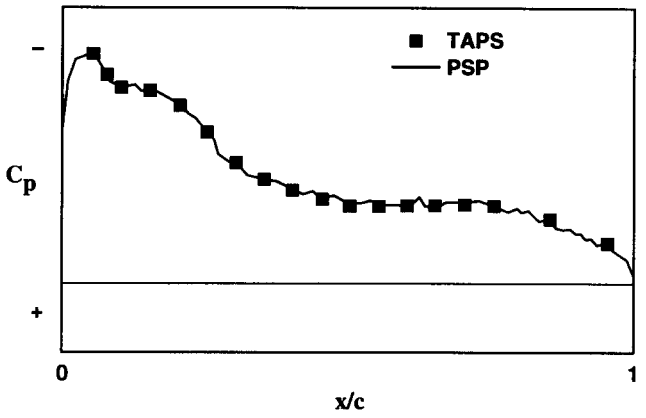


**Figure 13.** Comparison of chordwise pressure distributions obtained from PSP (solid line) and conventional pressure taps (symbols) at one spanwise location of generic transport wing: $M = 0.8$, $\alpha = 10°$.

visual pattern provided allows identification of features of interest such as shocks and their location and areas of high loading. Readily apparent are features in the pressure distribution that would be difficult to deduce from the usual discrete tap data. An example in the Fig. 14 data is the spanwise structure of the shock at higher angles of attack.

## INTRUSIVENESS (AN OPEN ISSUE)

The application of PSP coating to the model surface can alter the model's aerodynamic characteristics. Two mechanisms permit the coating to be intrusive. The first is a viscous effect, the surface finish of the coating, its roughness and waviness, altering the boundary layer. The second mechanism is inviscid, the coating displacement altering the model geometry (e.g., wing leading-edge radius).

At transonic Mach numbers, changes in the boundary layer can have a dramatic effect on shock location on the

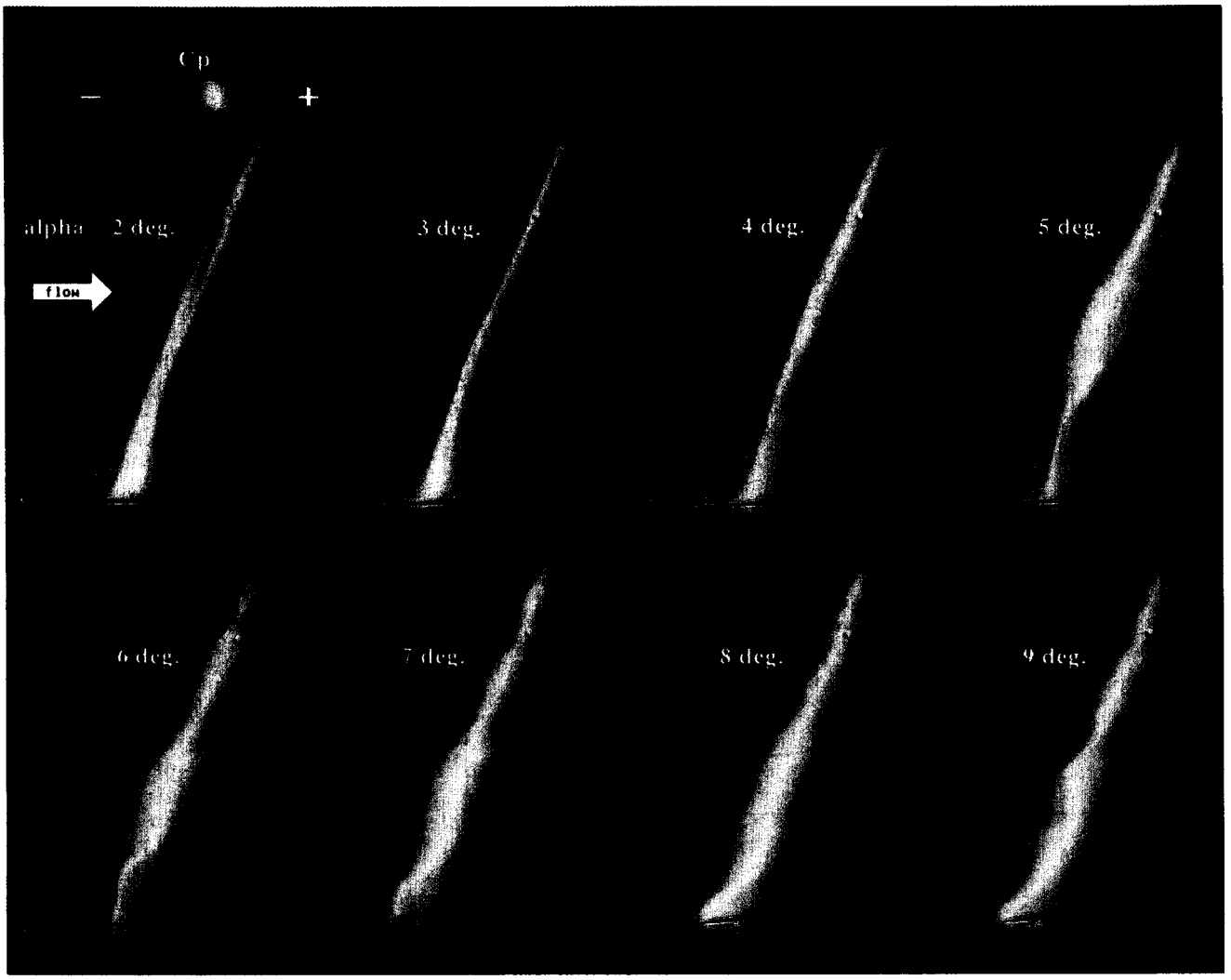


**Figure 14.** Composite of upper surface pressure maps showing variation of surface pressure with increasing angle of attack. Generic transport wing, $M = 0.8$. Color denotes pressure level: blue is high pressure, red is low pressure.

model surface. We have acquired data under transonic flow conditions that showed the movement of the shock location on a transport wing that can be attributed to the change in boundary layer thickness induced by the surface roughness of the PSP coating. This is illustrated in Fig. 15. Such experiences are not unique. Crites et al. [17] noted in a study of a 4.7% F-15 aircraft model a large change in its aerodynamic performance characteristics (lift, drag, and pitching moment) due to the addition of a PSP coating. Initially an increase of 65 drag counts in the minimum drag coefficient was found. Multiple paint applications were tried, and through careful application technique results were achieved that agreed well (within 2 drag counts) with the bare model. Obviously the "quality" of the paint application and the resulting surface finish is an important factor.

The addition of the PSP coating layer has been observed [5, 17] in some test situations to affect the pressure tap readings, introducing a bias error in the tap measurements relative to the clean no-paint condition. This bias error is a measurement uncertainty factor when the in situ calibration approach is employed.

## ADDITIONAL CONSIDERATIONS

In the typical operational testing environment, a number of additional complicating factors are introduced that are possible sources of error and are thus of concern. The first of these pragmatic factors arises from the unfortunate fact that all production level wind tunnels are "dirty" to some degree. The model surface [2] can become dusty during the time between acquisition of the wind-off and wind-on images. The result is an attenuation of the excitation radiation and emission signal that leads to measurement error. The flow will produce a nonuniform distribution of dust over the model surface. Wing leading edges are particularly prone to dust accumulation.

Further artifacts also result from this tunnel environmental quality problem. The PSP coating can be eroded away by particulates and grit in the tunnel flow. The PSP coating can also become chemically contaminated due to the presence of lubricants in the flow or even the skin oils left behind from handling the painted model surface. Mechanical durability and sensitivity to contamination are characteristics that vary a great deal between specific PSP coatings. In some facilities these characteristics can be a primary factor in PSP coating selection.

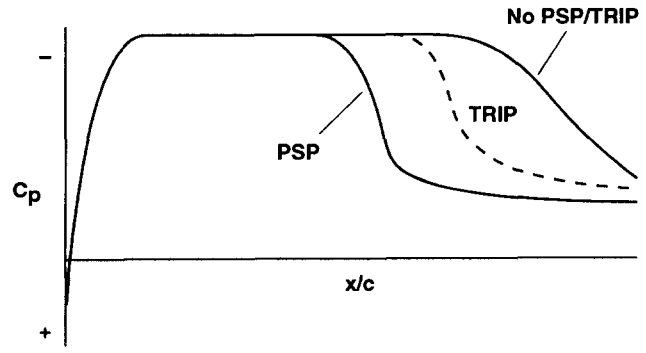


**Figure 15.** Example of aerodynamic intrusiveness: sketch of upper surface $C_p$ distribution of transport wing in transonic flow for bare wing (no PSP or boundary layer trip), bare wing with boundary layer trip, and PSP coated wing (no boundary layer trip).

Another complicating factor is reflection of the luminescence emission off the wind tunnel test section walls and, for full complex aircraft configurations, off other model components. The result of this self-illumination is a contamination of the detected signal. An example would be light emitted from the horizontal tail being reflected off the vertical tail and detected as part of the emission from that surface. Limited information exists in the literature on the magnitude of this problem. It is known from experience, however, that it is installation-dependent. Though hardly elegant, an effective solution to avoid it is to paint and acquire data from various model components separately.

## COMMENTS ON MEASUREMENT UNCERTAINTY

The unorthodox nature of the PSP method and the large number of variables inherent to the technique make it difficult to estimate the overall measurement uncertainty. Complications arise from the fact that in operational aerodynamic testing the measurement environment is far from ideal. In comparison to a controlled setting, the operational environment contains more error sources, some of them large, uncertain, and installation-dependent. To experimentally isolate the uncertainty of the PSP measurement that is specific to the PSP system alone is a formidable task.

A complete comprehensive error analysis has yet to be performed and reported that is suitable for estimating measurement uncertainty under practical operational conditions. An initial effort has been made by Sajben [21], who looked at the relative influence on measurement uncertainty of the most basic measurement quantities. He confirmed the previously held intuitive judgment that when the Stern–Volmer ratio approach is employed, precision is reduced at low Mach numbers and low pressures and precision is superior at moderate to high Mach numbers and moderate pressures. Surface temperature variations, depending on the PSP coating characteristics, were found capable of producing large measurement uncertainty levels. It is worth noting that Sajben found that the measurement uncertainty even in his simple model was sensitive to flow conditions, both free-stream and local, to such an extent that "a simple global characterization of error magnitude does not seem practical." Error estimates of a simplified form are also given by Bukov et al. [2], Crites et al. [17], and Morris et al. [18].

Some appreciation of the accuracy obtainable in practice is provided by comparison of PSP-derived pressures to simultaneous conventional pressure tap measurements. Under controlled static conditions, Morris et al. [18] reported a minimum pressure resolution (i.e., maximum conventional versus PSP difference) of 344 Pa (or 0.05 psi) at atmospheric pressure using PSP equipment equivalent to that in the generic transport example study described previously. For the transonic generic transport data reported in this paper, the overall rms pressure difference between PSP and taps was 1526 Pa (0.22 psi, or 1.5% of atmospheric pressure). In terms of pressure coefficient, the rms difference was 0.03. In a more recent large-scale

operational test at moderate supersonic Mach numbers, we were able to achieve an overall rms tap versus PSP difference of 344 Pa (or 0.05 psi). For the test in question this corresponded to an rms pressure coefficient difference of 0.01 between taps and PSP. This range of numbers is representative of that reported in the literature using PSP at transonic to supersonic Mach numbers. These levels will certainly be reduced in the near future. It must be noted that the wind tunnel environment where PSP is employed has not been modified to suit the PSP method and reduce error sources. The expanding user base for PSP will hopefully change this.

A determination of PSP measurement uncertainty from the above relative comparison requires a knowledge of the pressure tap measurement uncertainty. Unfortunately, and most surprisingly, such information is not openly or readily available for current tap measurement systems employed on aircraft configurations in operational large-scale testing environments. The uncertainty associated with the electronic pressure transducer, gleaned from the manufacturer's specifications, is what is usually provided by facility operators. This ignores the uncertainty of the entire "tap system" (i.e., the tap hole scale and geometry, flow conditions, tubing runs, and so on) of which the transducer is only one element. Variability in tunnel conditions is also a factor in this situation. The dearth of such information is primarily due to time and cost pressures in production testing and also to an historically based confidence in tap technology. Systematic studies are needed in a range of operational facilities and conditions, with the resulting information being made publicly available.

## Uncertainty Limit: Photon Shot Noise

The ultimate uncertainty limit in PSP measurements is set by photon shot noise arising from the quantum nature of light itself. This performance limit represents the "minimum uncertainty" that would be attained in an ideal situation with the perfect "zero" instrumentation noise measurement system. Photon shot noise is a random error source governed by Poisson statistics, which dictates that the standard deviation in the signal is equal to the square root of the mean of the signal. In familiar terms, this means that the shot noise signal-to-noise ratio (SNR) is equal to the square root of the mean of the number of photons received, and thus photoelectrons collected by the imaging system.

In most PSP test situations employing scientific grade CCD cameras, the measurement will be photon shot noise limited [2, 17, 18, 25]. Since the full well capacity (saturation limit) of the CCD determines how many photoelectrons can be gathered at a pixel in a single image, this quantity sets the optimum shot noise SNR of a single measurement. By summing a number of images, substantial improvements in shot noise–dominated SNR can be attained [2, 18]. Through image addition (or equivalent averaging), the shot noise SNR can be increased to the resolution limit set by camera readout and digitization noise. The same photoelectron gathering advantage can be obtained by summing adjacent pixels, though it results in a corresponding loss in spatial resolution.

## Low-Speed Situation: Photon Shot Noise Implications

Pressure-sensitive paint can be thought of as an absolute pressure sensor. This present intrinsic characteristic in conjunction with the Stern–Volmer ratio methodology has important consequences for PSP measurement uncertainty in low subsonic test applications of the method. At low Mach number conditions, the pressure, and corresponding light emission, difference between wind-off and wind-on conditions is relatively low compared to that which occurs at higher Mach numbers. Consequently, since the SNR of the measurement system is a fixed performance parameter, this results in increasing noise and thus uncertainty in the measurement as the Mach number decreases for a given test geometry.

Considering only photon shot noise, the following first-order approximation can be derived for uncertainty at low subsonic Mach numbers:

$$\Delta C_p \cong \frac{2}{BM^2\sqrt{mN}} \tag{7}$$

Here $\Delta C_p$ is the uncertainty (standard deviation) given in terms of the pressure coefficient, $M$ is Mach number, $B$ is the slope of the Stern–Volmer calibration curve at atmospheric pressure, $N$ is the CCD full-well capacity, and $m$ is the number of images acquired and summed. In the derivation of Eq. (7) it was assumed that the tunnel circuit is vented to standard atmospheric pressure at the test section or the plenum chamber. Equation (7) is approximately valid for $M < 0.4$.

Some appreciation of the difficulty of making accurate measurements at low subsonic speeds is provided in Fig. 16, where Eq. (7) has been used to plot uncertainty as a function of Mach number. A representative CCD full-well capacity, $N = 330{,}000$, is assumed and $B = 1.0$. As is evident, uncertainty in PSP measurements in the low-speed regime increases dramatically as the Mach number decreases. Also apparent is the benefit arising from image

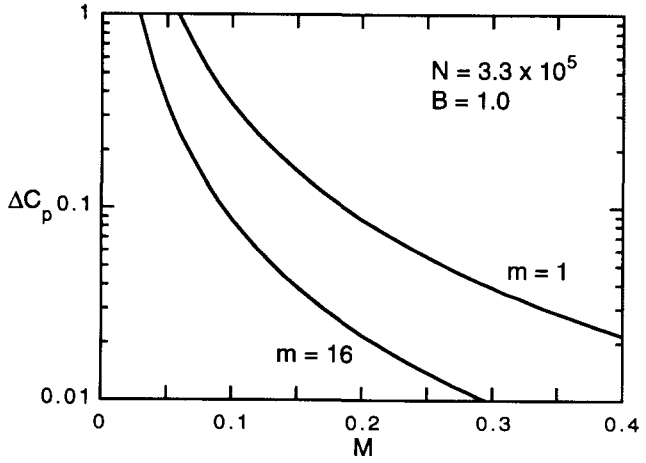


**Figure 16.** Low subsonic Mach number situation. First-order estimate of photon shot noise measurement uncertainty $\Delta C_p$, assuming that the tunnel is vented to the atmosphere; CCD full-well capacity, $N = 330{,}000$; linear Stern–Volmer calibration curve slope, $B = 1.0$.

frame addition (or averaging), the uncertainty decreasing as the square root of the number of images added.

## CONCLUDING REMARKS

An overall introduction to the PSP method has been provided, and the essential aspects of the technique have been described. The discussion was confined to the application of the technique to aircraft development testing, since at present, and historically, that is the development focus of the technology. We envision that in the future, the method will have an impact in a broad spectrum of applications in experimental fluid dynamics. Within aircraft development testing, the method has established itself as a powerful diagnostic tool. It has proven capable of producing quantitative data at high flow speeds where pressure differences of a suitable magnitude are produced and qualitative data over a broad speed range. The PSP method is not a mature technology. The great potential it holds, however, is firmly recognized by industry, and the technology is being developed at an extremely rapid pace. Improvements in accuracy, productivity, and capability are anticipated. Attainment of the method's full promise is entirely feasible and is not that far off in the future.

We are thankful to J. Espina for enlightening discussions on various aspects of PSP technology and his support of this effort. We also wish to thank Professor M. Gouterman and his research group for the data on PSP coating characteristics. Finally, B. G. M. wishes to dedicate this paper to the memory of his doctoral advisor and "guru" K. Karamcheti, a great teacher and human being. He is missed.

## NOMENCLATURE

$a$, $b$ transform coefficients, dimensionless

$A$, $B$, $C$ paint sensitivity coefficients, dimensionless

$c$ oxygen concentration within coating, $mol/m^3$

$C_D$ drag coefficient, dimensionless

$C_L$ lift coefficient, dimensionless

$C_p$ pressure coefficient, dimensionless

$\Delta C_p$ photon shot noise uncertainty in terms of $C_p$, dimensionless

$I$ luminescence intensity, wind-on, gray levels, $W/m^2$

$I_{max}$ maximum luminescence intensity value in absence of quencher, gray levels, $W/m^2$

$I_0$ luminescence intensity, wind-off, gray levels, $W/m^2$

$K$ Stern–Volmer quenching constant, $m^3/mol$

$M$ free-stream Mach number, dimensionless

$m$ number of image frames summed, dimensionless

$N$ CCD full-well capacity (pixel photoelectron saturation number), dimensionless

$P$ surface pressure, wind on, $N/m^2$

$P_0$ surface pressure, wind off, $N/m^2$

$S$ Henry's law (solubility) coefficient, $(mol/m^3)/(N/m^2)$

$t$ time, s

$T$ surface temperature, °C

$x$, $y$ image plane coordinates, wind off, dimensionless

$x'$, $y'$ image plane coordinates, wind on, dimensionless

$x/c$ airfoil chordwise coordinate, measured from leading edge, normalized with respect to chord, dimensionless

$X$ mole fraction of oxygen in air, dimensionless

### Greek Symbols

$\alpha$ geometric angle of attack, deg

$\lambda$ wavelength, nm

## REFERENCES

1. Ardasheva, M. M., Nevskii, L. B., and Pervushin, G. E., Measurement of Pressure Distribution by Means of Indicator Coatings, *Zh. Prikl. Mekh. Tekhn. Fiz.*, **26**(4), 24–30, 1985; translated into English in *J. Appl. Mech. Tech. Phys.*, **26**(4), 469–474, 1985.
2. Bukov, A. P., Orlov, A. A., Mosharov, V. E., Radchenko, V. N., Pesetsky, V. A., et al., Application of Luminescence Quenching for Pressure Field Measurements on the Model Surface in a Wind Tunnel, Proc. Wind Tunnels and Wind Tunnel Test Techniques Conf., Royal Aeronautical Society, London, U.K., pp. 8.1–8.11, September 1992.
3. Volan, A., and Alati, L., A New Optical Pressure Measurement System, Proc. 14th Int. Cong. Instrumentation in Aerospace Simulation Facilities (ICIASF), Institute of Electrical and Electronics Engineers, New York, pp. 10–16, 1991.
4. Engler, R. H., Hartmann, K., and Schulze, B., Aerodynamic Assessment of an Optical Pressure Measurement System (OPMS) by Comparison with Conventional Pressure Measurements in a High Speed Wind Tunnel, Proc. 14th Int. Congr. Instrumentation in Aerospace Simulation Facilities (ICIASF), Institute of Electrical and Electronics Engineers, New York, pp. 17–24, 1991.
5. Engler, R. H., Hartmann, K., Troyanovski, I., and Vollan, A., Description and assessment of a new optical pressure measurement system (OPMS) demonstrated in the high speed wind tunnel of DLR in Gottingen, DLR Report DLR-FB 92-24, October 1992.
6. McLachlan, B. G., Kavandi, J. L., Callis, J. B., Gouterman, M., Green, D., et al., Surface Pressure Field Mapping Using Luminescent Coatings, *Exp. Fluids*, **14**(1/2), 33–41, 1993. Presented at 42nd Meeting of the American Physical Society, Division of Fluid Dynamics, Palo Alto, CA, November 1989. *Bull. Am. Phys. Soc.*, **34**(10), November 1989.
7. Kavandi, J., Callis, J., Gouterman, M., Khalil, G., Wright, D., et al., Luminescent Barometry in Wind Tunnels, *Rev. Sci. Instrum.*, **61**(5), 3340–3347, 1990.
8. Kavandi, J. L., Luminescence Imaging for Aerodynamic Pressure Measurements, Ph.D. Thesis, Chemistry Dept., Univ. Washington, Seattle, WA, 1990.
9. McLachlan, B. G., Bell, J. H., Kennelly, R. A., Schreiner, J. A., Smith, S. C., et al., Pressure Sensitive Paint Use in the Supersonic High-Sweep Oblique Wing (SHOW) Test, AIAA Paper No. 92-2686, AIAA 10th Applied Aerodynamics Conf., Palo Alto, CA, June 1992.
10. McLachlan, B. G., Bell, J. H., Espina, J., Gallery, J., Gouterman, M., et al., Flight Testing of a Luminescent Surface Pressure Sensor, NASA TM-103970, October 1992.
11. Bell, J. H., and McLachlan, B. G., Image Registration for Luminescent Paint Sensors, AIAA Paper No. 93-0178, AIAA 31st Aerospace Sciences Meeting, Reno, NV, January 1993.
12. Gallery, J., Gouterman, M., Callis, J., Khalil, G., McLachlan, B. G., et al., Aerodynamic Temperature Measurements by Luminescence Imaging, *Rev. Sci. Instrum.*, **65**(3), 712–720, 1994.
13. Gallery, J. M., Luminescence Imaging for Aerodynamic Temperature and Pressure Measurements, Ph.D. Thesis, Chemistry Dept., Univ. Washington, Seattle, WA, 1993.

14. McLachlan, B. G., and Bell, J. H., Boundary Layer Transition Detection by Luminescence Imaging, AIAA Paper No. 93-0177, AIAA 31st Aerospace Sciences Meeting, Reno, NV, January 1993.
15. Uibel, R. H., Khalil, G., Gouterman, M., Gallery, J., and Callis, J. B., Video Luminescent Barometry: The Induction Period, AIAA Paper No. 93-0179, AIAA 31st Aerospace Sciences Meeting, Reno, NV, January 1993.
16. Baron, A. L., Danielson, J. D. S., Gouterman, M., Wan, J. R., Callis, J. B., et al., Submillisecond Response Times of Oxygen-Quenched Luminescent Coatings, *Rev. Sci. Instrum.*, **64**(12), 3394–3402, 1993.
17. Crites, R. C., Benne, M. E., Morris, M. J., and Donovan, J. F., Optical Surface Pressure Measurement: Initial Experience in the MCAIR PSTWT, Proc. Wind Tunnels and Wind Tunnel Test Techniques Conf., Royal Aeronautical Society, London, U.K., pp. 9.1–9.13, September 1992.
18. Morris, M. J., Benne, M. E., Crites, R. C., and Donovan, J. F., Aerodynamic Measurements Based on Photoluminescence, AIAA Paper No. 93-0175, AIAA 31st Aerospace Sciences Meeting, Reno, NV, January 1993.
19. Donovan, J. F., Morris, M. J., Pal, A., Benne, M. E., and Crites, R. C., Data Analysis Techniques for Pressure- and Temperature-Sensitive Paint, AIAA Paper No. 93-0176, AIAA 31st Aerospace Sciences Meeting, Reno, NV, January 1993.
20. Morris, M. J., Donovan, J. F., Kegelman, J. T., Schwab, S. D., Levy, R. L., et al., Aerodynamic Applications of Pressure-Sensitive Paint, *AIAA J.*, **31**(2), 419–425, 1993.
21. Sajben, M., Uncertainty Estimates for Pressure Sensitive Paint Measurements, *AIAA J.*, **31**(11), 2105–2110, 1993.
22. Sellers, M. E., and Brill, J. A., Demonstration Test of Pressure Sensitive Paint in the AEDC 16-ft Transonic Wind Tunnel Using the TST Model, AIAA Paper No. 94-2481, 18th AIAA Aerospace Ground Testing Conf., Colorado Springs, CO, June 1994.
23. Parker, C. A., *Photoluminescence of Solutions*, Elsevier, Amsterdam, 1968.
24. Rogers, C. E., Permeation of Gases and Vapours in Polymers, in *Polymer Permeability*, J. Comyn, Ed., Chap. 2, Elsevier, London, 1985.
25. Dereniak, E. L., and Crowe, D. G., *Optical Radiation Detectors*, Wiley, New York, 1984.

Received August 5, 1994; revised November 28, 1994